



UNIVERSITY OF LEEDS

This is a repository copy of *A reconstitution method for integral membrane proteins in hybrid lipid-polymer vesicles for enhanced functional durability*.

White Rose Research Online URL for this paper:
<http://eprints.whiterose.ac.uk/126802/>

Version: Accepted Version

Article:

Seneviratne, R, Khan, S, Moscrop, E et al. (4 more authors) (2018) A reconstitution method for integral membrane proteins in hybrid lipid-polymer vesicles for enhanced functional durability. *Methods*, 147. pp. 142-149. ISSN 1046-2023

<https://doi.org/10.1016/j.ymeth.2018.01.021>

Copyright (c) 2018 Elsevier Inc. Licensed under the Creative Commons Attribution-Non Commercial No Derivatives 4.0 International License (<https://creativecommons.org/licenses/by-nc-nd/4.0/>)

Reuse

This article is distributed under the terms of the Creative Commons Attribution-NonCommercial-NoDerivs (CC BY-NC-ND) licence. This licence only allows you to download this work and share it with others as long as you credit the authors, but you can't change the article in any way or use it commercially. More information and the full terms of the licence here: <https://creativecommons.org/licenses/>

Takedown

If you consider content in White Rose Research Online to be in breach of UK law, please notify us by emailing eprints@whiterose.ac.uk including the URL of the record and the reason for the withdrawal request.



eprints@whiterose.ac.uk
<https://eprints.whiterose.ac.uk/>

A reconstitution method for integral membrane proteins in hybrid lipid-polymer vesicles for enhanced functional durability

Rashmi Seneviratne¹, Sanobar Khan¹, Ellen Moscrop¹, Michael Rappolt², Stephen P. Muench³,
Lars J.C. Jeuken³ and Paul A. Beales^{1,*}

¹ School of Chemistry and Astbury Centre for Structural Molecular Biology, University of Leeds, Leeds, UK

² School of Food Science and Nutrition, University of Leeds, Leeds, UK

³ School of Biomedical Sciences and Astbury Centre for Structural Molecular Biology, University of Leeds, Leeds, UK

* Corresponding author: p.a.beales@leeds.ac.uk

Abstract

Hybrid vesicles composed of lipids and block copolymers hold promise for increasing liposome stability and providing a stable environment for membrane proteins. Recently we reported the successful functional reconstitution of the integral membrane protein cytochrome bo_3 (ubiquinol oxidase) into hybrid vesicles composed of a blend of phospholipids and a block copolymer (PBd-PEO). We demonstrated that these novel membrane environments stabilise the enzymes' activity, prolonging their functional lifetime [Chem Commun. 52 (2016) 11020-11023]. This approach holds great promise for applications of membrane proteins where enhanced durability, stability and shelf-life will be essential to creating a viable technology. Here we present a detailed account of our methods for membrane protein reconstitution into hybrid vesicles and discuss tips and challenges when using block copolymers compared to pure phospholipid systems that are more common materials for this purpose. We also extend the characterisation of these hybrid vesicles beyond what we have previously reported and show: (i) hybrid membranes are less permeable to protons than phospholipid bilayers; (ii) extended enzyme activity data is presented over a period of 500 days, which fully reveals the truly remarkable enhancement in functional lifetime that hybrid vesicles facilitate.

Introduction

The case for the importance and prevalence of membrane proteins and the challenges associated with their study and application is well established [1-3]. These arguments include their prevalence within the proteome, as pharmaceutical targets and their wide-ranging functional properties, including signalling, catalysis, adhesion and transport. The challenges associated with handling membrane proteins *ex vivo* fundamentally comes down to their instability in an isotropic solvent such as water, requiring amphiphilic (liquid crystalline) solvation mimicking their natural environment of a lipid bilayer [4]. Numerous self-assembling amphiphilic soft materials, e.g. micelles, vesicles and cubic phases, have been used in the handling and manipulation of membrane proteins [5]. Significant recent advances have been made in embedding membrane proteins within discoidal nanoparticles [6-8]; while these systems have their advantages in the appropriate context, discotic systems do not provide the compartmentalised architecture of a living cell. Here, our focus is on vesicular structures that contain a distinct aqueous lumen separated from the bulk environment.

The classical vesicle for membrane protein reconstitution is the liposome due to its close resemblance to the natural bilayer architecture and chemistry of a living cell membrane [9]. However, the precise properties of native membranes are difficult to fully replicate in synthetic systems: e.g., transbilayer compositional asymmetry [10], transient nanoscale “raft” domains [11, 12], crowding from high membrane protein content [13, 14], and the scaffolding effects of cytoskeletal networks [15, 16]. All of these features have the potential to influence the function and stability of integral proteins through modulation of physicochemical properties such as fluidity, mechanics and lateral pressure profile. Consequently, these intricacies are suggestive of desirable modifications that could further mimic the natural membrane environment.

One well-established weakness of synthetic liposomes is the fluidity of the lipid bilayer that leads to long-term structural instabilities: its dynamic and labile nature can lead to formation of transient pores and membrane rupture [17-19]. Further known ageing phenomena in liposomes can include slow aggregation and agglomeration processes, and gradual oxidative damage of the lipids (and also of any integral proteins). The stable lifetime of the liposome therefore has an impact on the stability of proteins embedded within its structure. Vesicles formed from amphiphilic polymers (polymersomes) provide a broader parameter space in molecular size and chemistry than exists within natural lipids and can be designed for much enhanced stability compared to their lipid counterparts [20, 21]. Despite their unnatural structure (e.g. increased membrane thickness), chemistry (e.g. silicones) and differences in material properties such as rigidity and fluidity, some membrane proteins have been successfully reconstituted within polymersomes [22]. However, many membrane proteins can be challenging to functionally reconstitute, making unnatural polymersomes limited in their breadth of application within the membrane protein field [23].

Our solution to these challenges is through compromise. By forming hybrid vesicles composed of lipids and block copolymers, we can minimise the fragility of liposomes and the low biocompatibility of polymersomes by synergistically combining the best features of these systems and off-setting their weaknesses [24, 25]. Numerous examples of hybrid vesicles and their material properties have been reported [26-33], but only very recently have membrane proteins been introduced into these systems [23]. In a short communication, we described the enhanced functional lifetime of a respiratory enzyme, cytochrome bo_3 (ubiquinol oxidase), reconstituted within a hybrid vesicle compared to a conventional proteoliposome [34]. It is known that the incorporation of block copolymers within hybrid vesicles reduces membrane fluidity and enhances their mechanical properties (e.g. increased toughness and lysis strain) [25]. Speculatively, these changes in membrane properties may be more native-like (as discussed above) and, alongside enhanced macromolecular crowding in the membrane from these polymers, contribute to improving the function and stability of its integral proteins. We believe that this approach will have diverse applications for enhancing the functional durability of reconstituted membrane proteins.

Here we give a detailed account of our reconstitution method successfully employed for cytochrome bo_3 within hybrid vesicles (Fig. 1) and aim to provide the community with insights gained from our experience working with hybrid lipid/block copolymer systems with regards to how other common approaches to membrane protein constitution within liposomes may or may not be easily adapted to a hybrid vesicle. Finally, we extend the material characterisation we have previously reported for cytochrome bo_3 in hybrid vesicles by determining membrane permeability to protons and significantly extending the period over which the enzyme function is monitored from 42 days to approximately 500 days. These updated results profoundly emphasise the power of our approach in enhancing the functional durability of this protein.

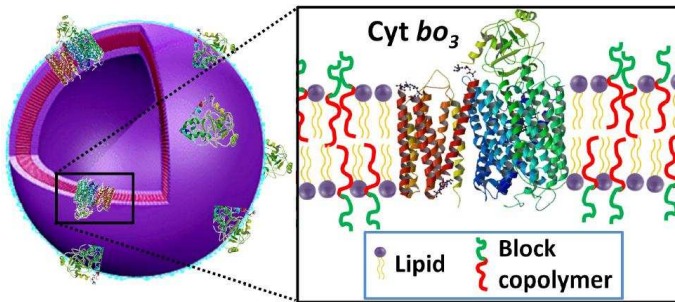


Figure 1. Integral membrane proteins (e.g. cytochrome bo_3) reconstituted in a hybrid vesicle with membranes composed of a blend of phospholipids and amphiphilic diblock copolymers.

Method for membrane protein reconstitution

Below we give a detailed step-by-step guide to our method for cytochrome bo_3 reconstitution within hybrid POPC/PBd₂₂-b-PEO₁₄ vesicles. The method is summarised in the flow chart in Fig. 2. This method is adapted from the reconstitution protocol reported by Geertsma et al. [35]. Note that we have not optimised all parameters in the protocol and so this should be treated as a starting point for adaption to the use of other proteins.

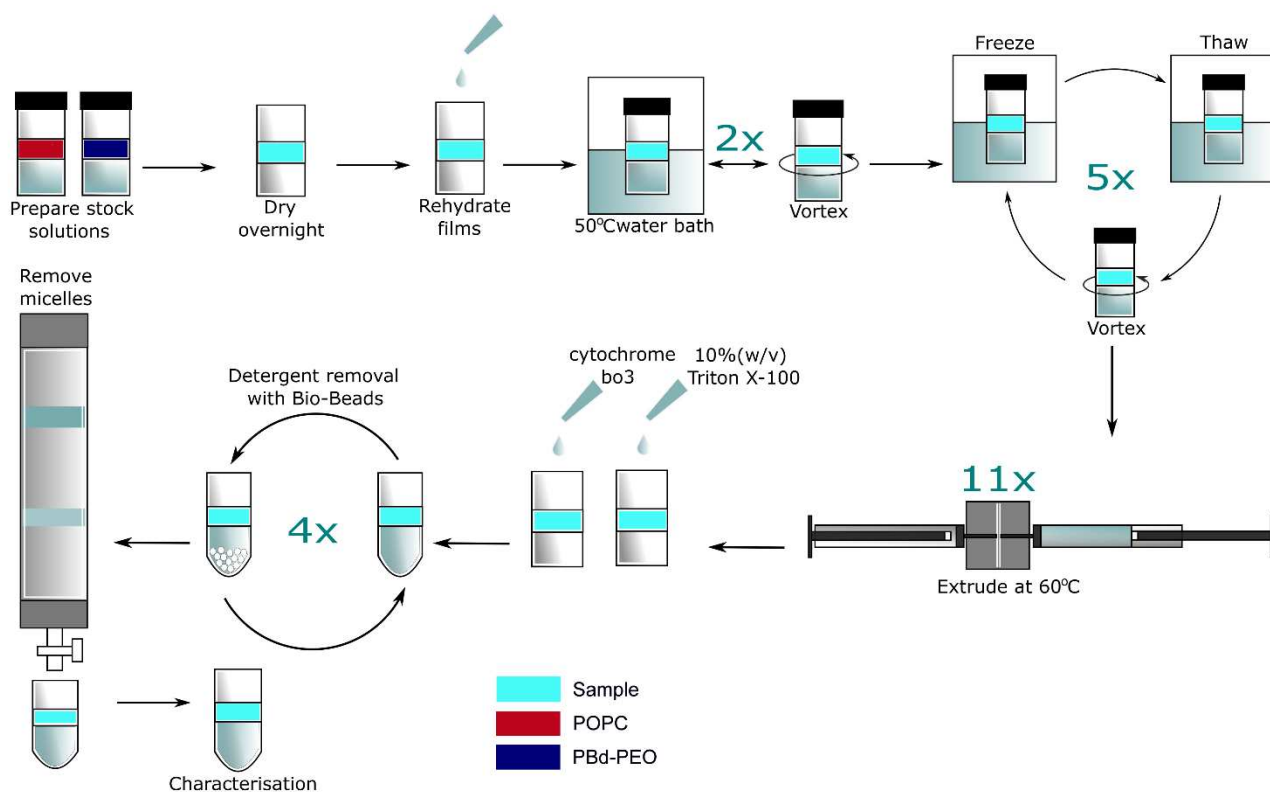


Figure 2. Diagrammatic workflow chart of our reconstitution method for generating hybrid vesicles incorporating membrane proteins.

1. Measure 0.01183 g of Poly(butadiene-*b*-ethylene oxide) (PBd₂₂-*b*-PEO₁₄; Polymer Source, P9089-BdEO) and add 1.0 mL of chloroform using a glass Hamilton syringe to give 1.0 mL (6.57mM) stock solution. All chloroform solutions are made in glass vials.
2. To generate different hybrid vesicle compositions, the relative volumes of stock solution for 1-palmitoyl-2-oleoyl-*sn*-glycero-3-phosphocholine (POPC; 25 mg/mL, Avanti Polar Lipids, CAS no. 26853-31-6) and PBd-PEO are measured using a Hamilton syringe and mixed in a glass vial using the values given in Table 1.

Table 1. Volumes of POPC and PBd-PEO stock solutions in chloroform mixed to create the different hybrid vesicle compositions (mol%) studied.

Sample (PBd-PEO mol%)	POPC volume (μL)	PBd-PEO volume (μL)
0%	200	0
25%	150	250
50%	100	500
75%	50	750
100%	0	1000

3. If purification by size exclusion chromatography will be required add 42 μL (0.5 mol%) of 1,2-dioleoyl-sn-glycero-3-phosphoethanolamine-N-(lissamine rhodamine B sulfonyl) (ammonium salt) (Rh-DOPE; 1 mg/mL Avanti Polar Lipids; CAS no. 384833-00-5) in chloroform (this aids visual tracking of vesicle fractions down the column).
4. Solutions are dried overnight under vacuum in a desiccator to give a lipid/polymer film. (Note that we see no reason why commonly used 2-4 h solvent evaporation times are not feasible here; the overnight step fits our preferred workflow.)
5. The films are rehydrated with 1.0 mL of aqueous buffer containing 20 mM 4-(2-hydroxyethyl)-1-piperazineethanesulfonic acid (HEPES), 10 mM sodium chloride at pH 7.4.
6. The rehydrated films are incubated at 50 $^{\circ}\text{C}$ for 5 minutes and vortex ed for 1 minute, twice, or until the dried film is fully resuspended in solution (see tip #1 for further discussion).
7. Suspensions are then frozen in liquid nitrogen, thawed in a 60 $^{\circ}\text{C}$ water bath and vortexed for 10 seconds. This cycle is repeated 5 times.
8. Suspensions are extruded 11 times through a 100 nm pore size polycarbonate membrane filter using an Avanti Mini-Extruder with heating block on a hotplate at 60 $^{\circ}\text{C}$ to form nanovesicles. The elevated temperature makes samples easier to extrude.
9. With an independent sample from the one to be used for protein reconstitution, detergent destabilisation profiles for the samples are obtained by titrating 1000 μL of vesicles (6.57 mM) with 1.0 μL aliquot additions of 10% (w/v) Triton X-100 (Sigma-Aldrich, CAS no. 9002-93-1) while observing the optical density at 540 nm until the suspensions go from a translucent to clear appearance. The destabilisation point is just after the optical density peak, just as the profile begins to rapidly decrease. Using the peak as the destabilisation point gives a lower probability of reconstitution. For some compositions, a clear peak is not observed: see tip #4 for further discussion. For reference, we have previously reported our titration curves for different hybrid vesicle compositions in supplementary figure S2 of Khan et al. [34].
10. To reconstitute the membrane protein, the prepared 1.0 mL of vesicles are destabilised using the observed destabilisation volume of 10% (w/v) Triton X-100 determined in step 9. To 500 μL of destabilised vesicles, 10 μg (approx. 10 μL , 6.88 μM) of purified cytochrome b_0_3 (20 mM Tris.Cl, 5 mM MgSO_4 , 100 mM NaCl, 5% glycerol, 0.05% DDM) is added and allowed to inoculate on a rocker for 15 min at 4 $^{\circ}\text{C}$. Note that details of cytochrome b_0_3 expression and purification are described in the additional methods below.
11. To each 500 μL solution from step 10, 20 mg of Bio-Beads (Bio-Beads SM-2 adsorbents, Bio-Rad) is added and the samples are incubated on a rocker at 4 $^{\circ}\text{C}$. There are 4 successive cycles in total: Cycle1 = 20 mg Bio-Beads, incubated for 30 min; Cycle 2 = 20 mg Bio-Beads, incubated for 1 h; Cycle 3 = 20 mg Bio-Beads, incubated for 6 h; Cycle 4 = 20 mg Bio-Beads, incubated for 6 h.
 - a. For each cycle the sample is pipetted from the previous Eppendorf sample tube into a new tube containing fresh Bio-Beads.
 - b. Detergent removal is completed over 2 days: Cycles 1, 2 and 3 takes place on day 1 and cycle 4 takes place on day 2. Between Cycles 3 and 4 the samples are kept in tubes without Bio-Beads.
12. The particle size distributions in 0.5 mL fractions are measured by dynamic light scattering. If a monomodal size distribution is found centred near 100 nm hydrodynamic diameter then

the preparation protocol can be stopped here. If not, purification of vesicles may be required (steps 13 and 14), before continuing to step 15. See tip #5 for further discussion.

13. The nanovesicle samples are run on a Sephadex G50 column under gravity using 20 mM HEPES and 10 mM sodium chloride buffered to pH 7.4 as the mobile phase. See tip #6 for a discussion of vesicle purification methods.
 - a. The presence of Rh-DOPE allows the vesicles to be visually tracked on the column.
 - b. 0.5 mL fractions are collected and quantified by UV-vis adsorption spectroscopy at 570 nm to measure the Rh-DOPE content.
14. The 0.5 mL fractions from step 13 containing Rh-DOPE are characterised using dynamic light scattering for particle size distribution to confirm the presence of purified vesicles (a single monomodal peak centred near 100 nm diameter).
15. Proteo-hybrid vesicles can now be further analysed for protein activity, for example using an ubiquinol assay or an HPTS assay as discussed in the additional methods section below.

Trouble-shooting, tips and other considerations when using block copolymers

While many of the same vesicle preparation methods that can be used for phospholipid systems can also be successfully adapted when using block copolymers, block copolymer systems have many properties that are very distinct to lipid systems and these need to be taken into consideration when designing and optimising hybrid vesicle reconstitution protocols:

1. Slower molecular dynamics. Viscosity of block copolymer films and their slower molecular dynamics within aggregate structures mean that the timescales you may be accustomed to using for various vesicle preparation steps with phospholipids, may need to be significantly extended. For example, dispersion of dried lipid/polymer films into aqueous media can be much slower and require heating of the media to facilitate full suspension of the polymer/lipid film. This can be monitored visually during sample preparation. An alternative approach is slow hydration of the film with gentle mixing for 1-2 days, permitting the film to slowly disperse into solution. The advantage of gentle hydration is that this gives time for the polymer to assemble into equilibrium structures (vesicles); forcing the polymer/lipid film quickly into solution through heating and sonication can lead to the formation of kinetically-trapped micellar structures coexisting with the vesicle population for some polymer:lipid mixing ratios. However, this is not necessarily a major problem as discussed in more detail below.
2. Frustrated micelle to vesicle transition. Several reported methods for membrane protein reconstitution within liposomes start with the lipids being mixed with detergent in the micellar state before triggering a micelle to vesicle transition in the presence of the membrane protein by detergent removal. In our hands, we have not been able to successfully reproduce such a micelle to vesicle transition for hybrid mixtures of POPC and PBd₂₂-PEO₁₄ (or for PBd₂₂-PEO₁₄ polymersomes). Polymer/lipid mixtures were micellised with 55 mM Octyl β-D-glucopyranoside (OGP; Sigma-Aldrich, CAS no. 29836-26-8) or with 40mM sodium cholate hydrate (Alfa Aesar, CAS no. 206986-87-0). We attempted vesicle formation by detergent removal using BioBeads and by dialysis; while these were unsuccessful for polymer-containing samples, both methods were successful for lipid-only positive control samples. Our interpretation of this is that the much slower dynamics of molecules within block copolymer assemblies frustrates the micelle to vesicle transition, leaving block copolymer-rich assemblies kinetically trapped in the micellar state. It should be noted that detergent-assisted polymersome formation has been reported for peptide block copolymers and a

larger PBd₄₆-PEO₃₀ block copolymer using the same detergents that we tested [36]. Therefore, this approach should not be entirely dismissed, but careful optimisation may be required.

3. Buoyant vesicles. Some reconstitution methods use rapid dilution below the critical micelle concentration of the detergent followed by centrifugation for proteoliposome formation and purification. This method does not work when using PBd₂₂-PEO₁₄. While liposomes are slightly denser than water and can be pelleted by centrifugation, the polymersomes are less dense than water and float when centrifuged. Other block copolymer types might form vesicles of higher density, but it is helpful to be aware of this potential pitfall before embarking on this strategy.
4. Resistance to detergent-induced swelling. The detergent destabilisation method we use, detailed above, requires characterisation of the volume of Triton X-100 required before addition of the membrane protein. This is dependent on the composition of the hybrid membrane and so should not be taken to be a constant parameter. The concentration is determined by titration of the detergent into a vesicle sample of known concentration and monitoring turbidity by adsorption spectroscopy. Liposome samples initially increase in turbidity as the vesicles swell before the turbidity decreases due to membrane destabilisation, making the point of detergent-induced membrane disruption clear [35]. However, for samples containing block copolymers, detergent-lipid-polymer interactions are more complex. These vesicles do not visibly swell (no increase in turbidity) before the detergent concentration reaches a critical point and the vesicles break down. The point of instability can be more ambiguous in hybrid vesicles and so it is helpful to correlate desired detergent additions across different compositions of hybrid vesicles in order to select the most consistent detergent volume, which needs to be added to the samples.
5. Sample polymorphism. We have previously found that mixed samples of micelles and vesicles sometimes form during preparation of proteo-hybrid vesicles. This can be checked routinely by dynamic light scattering, where number- or volume-weighted size distributions should be analysed: intensity distributions greatly over-emphasize the abundance of larger structures (due to a dependence on the sixth power of particle size) and hide the existence of smaller micelle distributions in the sample. Cryo-Transmission Electron Microscopy is a useful approach if you wish to gain more detailed insight into the distribution of aggregate size, shape and morphology within samples, but is not ideal as a routine diagnostic characterisation tool for making decisions during sample preparation due to the time and complexity involved in sample preparation and imaging [37].
6. Purification of vesicles from other structural morphologies. We have previously demonstrated that vesicle fractions can be successfully purified from the coexisting micelles by size exclusion chromatography. Alternative approaches have also been reported for separation of vesicles and micelles, including flow-field fractionation and density-gradient centrifugation [38]. We have no experience with these alternative techniques and how they might impact upon membrane protein stability, but we also see no compelling reasons why these alternative approaches could not also prove successful. Indeed, under some circumstances, alternative separation strategies may prove superior to size exclusion chromatography.

Additional methods

Below we describe additional methods used for experiments reported in this manuscript: membrane protein expression and purification, proton permeability measurements and a functional assay based on the spectroscopic monitoring of decylubiquinol oxidation.

Ubiquinol oxidase expression and purification

Cytochrome bo_3 expression and purification was carried out following methods previously described in detail by Rumbley et al. [39]. We outline the approach below.

Cytochrome bo_3 is expressed from GO105/pJRhisA: a colony of transformed E. coli GO105 strain is inoculated incubated overnight at 37 °C / 200 RPM and used as a starter culture. LB media supplemented with 0.1 mg/mL carbenicillin and 0.1 mM $CuSO_4$ is inoculated with 2% starter culture and incubated again at 37 °C / 200 RPM in baffled flasks until the Optical Density (OD) measured at 600 nm (OD_{600}) reached 2.0 (~ 6 hours).

The cells are harvested by low speed centrifugation (7 kRCF, 10 min) and the pellets collected and resuspended in W1 buffer (0.25 g cells/mL, 20 mM MOPS, pH 7.4, 5 mM $MgSO_4$, 30 mM Na_2SO_4). The cells are lysed by passing them twice through a cell disruptor (Constant Systems) at 35 kPsi. The lysate is centrifuged (17.5 kRCF, 10 min) to remove unbroken cells, outer membranes, cell walls and any possible inclusion bodies. The supernatant is then centrifuged again (200 kRCF, 1 h, 4 °C) and the resultant pellet (membrane fraction) is resuspended in W1 buffer. The protein concentration is determined by BCA assay. The membrane fraction is then diluted to 3 – 4 mg/mL in solubilisation buffer (20 mM Tris.Cl, 5 mM $MgSO_4$, 300 mM NaCl, 20 mM imidazole, 10% glycerol, 1% DDM) and incubated for 1 h at 4 °C. The supernatant is centrifuged again (200 kRCF 1 h, 4 °C) to remove non-solubilised protein or other cellular components.

GO105/pJRhisA expresses cytochrome bo_3 with a polyhis-tag on subunit 2. Purification is performed with affinity chromatography with Ni^{2+} -nitrilotriacetic acid (NTA) resin (Super Ni-NTA Agarose, Generson). The resin is washed in batch with water (MilliQ, 18.2 M Ω cm) and then equilibrated with equilibration buffer (20 mM Tris/HCl, pH 8.0, 5 mM $MgSO_4$, 10% glycerol, 250 mM NaCl, 5 mM imidazole, 0.05% DDM). The equilibrated resin is mixed with the solubilised membrane protein and incubated on a Spiramix for 1 hour at 4 °C. After packing the resin in a column, the resin is washed with 10 column volumes of wash buffer (same as equilibration buffer, but with 40 mM imidazole). Cytochrome bo_3 is eluted with 10 column volumes elution buffer (20 mM Tris/HCl, pH 8.0, 5 mM $MgSO_4$, 10% glycerol, 100 mM NaCl, 200 mM imidazole, 0.05% DDM) Using ultrafiltration (100 kDa cut-off filter, Vivaspin, Satorius), the eluted cytochrome bo_3 is concentrated, while the buffer is exchanged to storage buffer (20 mM Tris/HCl, pH 8.0, 5 mM $MgSO_4$, 100 mM NaCl, 5% glycerol, 0.05% DDM). In Rumbley et al. [39] it is noted that imidazole needs to be removed prior to snap freezing and storage as imidazole can extract the copper ion from the active site of cytochrome bo_3 . The final purified protein sample concentration is determined quantitatively using the absorption of Soret band and BCA assay techniques. A SDS-PAGE and Western Blot are carried out on the samples taken throughout the purification process to confirm that the purification proceeded as expected and the final protein sample is pure (>90%).

Proton permeability measurements

5.244mg of 8-Hydroxypyrene-1,3,6-trisulfonic acid trisodium salt (HPTS, Sigma Aldrich, CAS no. 6358-69-6) is added to the 1.0 mL of rehydration buffer solution (step 5 in our reconstitution protocol above) to give 10 mM HPTS concentration, 40 mM HEPES and 20 mM NaCl. The rest of the reconstitution protocol is followed, without steps 3 (Rh-DOPE addition), 9-11 (protein reconstitution) and with step 13 (size exclusion chromatography) included to remove non-encapsulated HPTS. The encapsulation of HPTS allows the vesicles to be visually tracked on the column using a Sephadex G50 column under gravity.

To measure the proton permeability, the adsorption spectrum of 2 mL HPTS-encapsulated vesicles (~2 mM lipid/polymer) is measured using a UV-vis spectrometer scanning between 405 and 450 nm. To this, either 23 μ L of 1.0 M NaOH or 18 μ L of 1.0 M HCl is added to adjust the pH of the extraventricular solution to pH 8 or pH 7 respectively and the absorbance (between 405 and 450 nm) is monitored overnight; the first cycle scans are taken every minute over 2 hours and for the second

cycle scans are taken every 10 minutes for 7 hours with constant stirring. After this, 100 μL of 10% (w/v) Triton X-100 is added to completely destabilise the vesicles and release encapsulated HPTS (so that these probes experience the pH of the extravascular medium) before a final scan between 405 and 450 nm is completed.

A calibration curve using buffers ranging from pH 4 to pH 10 with 0.5 mM HPTS is used to determine the pH inside the encapsulated vesicles. The absorbance ratio of 450 to 405 nm is plotted against pH and the data fitted to find the relationship between them. Scattering effects are taken into account by adding empty POPC vesicles to each buffer solution.

The absorbance ratio between 450 and 405 nm (A_{450}/A_{405}) is converted to pH using the calibration curve. The pH is then plotted against time to show how pH changes with addition of NaOH (or HCl) and Triton X-100. Permeability coefficients are calculated using a methods recently reported for hybrid vesicles [40]. The pK_a (7.5) of HEPES is converted to a K_b value (-0.8129), which is then used to determine a formula to find the hydroxide ion and HEPES concentration of the sample throughout the experiment:

$$K_b = \frac{[OH^-] \times [HEPES]}{[HEPES^-]}$$

The flux of protons and hydroxide ions, J , was determined using the equation

$$J_{initial} = \frac{[OH^-]_{t=0} + [HEPES^-]_{t=1500} - [HEPES^-]_{t=0}}{\Delta t} \times \frac{V_{average}}{S_{average}}$$

Where $V_{average}$ is the internal volume and $S_{average}$ is the external surface area as determined by values obtained using Dynamic Light Scattering. $J_{initial}$ uses the amount of OH^- ions at $t = 0$ s present while J_{final} uses the amount of OH^- ions present at $t = 1500$ s. The net flux of protons and hydroxide ions, $J_{H^+/-OH^-}$, can be found by subtracting $J_{initial}$ from J_{final} . To find the permeability constant, P , the net flux, $J_{H^+/-OH^-}$, is divided by the hydroxide ion concentration gradient formed from the addition of NaOH (or HCl).

The deviations in actual pH (from a pH meter) and apparent pH (from the HPTS calibration curve) were corrected by offsetting the pH such that the initial pH for all experiments was the measured pH of the loading buffer. This is thought to be due to the interactions between HPTS and the vesicle material, for some vesicle systems. As the pH for these experiments are within the linear region of the calibration graph, all the data points can be offset by the same value for each series.

To measure net proton pumping across vesicle membranes due to the activity of cytochrome bo_3 , vesicle preparation and reconstitution is conducted according to our protocol using a reconstitution buffer of 10 mM HPTS concentration, 40 mM HEPES and 20 mM NaCl. Step 3 (Rh-DOPE addition) is not required as HPTS can be used to track vesicles in SEC (step 13), which removes excess HPTS from the extravascular medium. The adsorption spectrum of HPTS-encapsulated vesicles is again measured using a UV-vis spectrometer scanning between 405 and 450 nm. Decylubiquinol ($DUQH_2$) is then added and the vesicles are scanned again every 15 seconds over 3 minutes. The adsorption ratio (A_{450}/A_{405}) is converted using a calibration curve to intravesicular pH.

Functional Assay

Decylubiquinone (DUQ; Sigma-Aldrich, CAS No: 55486-00-5), is solubilised in absolute ethanol. The concentration is confirmed using UV-vis spectroscopy at 275 nm (where $\epsilon_{275nm} = 19 \text{ mM}^{-1} \text{ cm}^{-1}$ in absolute ethanol) to be approximately 2 mM. For the assay decylubiquinone (DUQ) is reduced to decylubiquinol ($DUQH_2$) using a crystal of sodium borohydride, so the appearance changes from yellow to colourless. The crystal is then removed and the excess hydride ions are removed by adding 1.0 μL of 0.1 M HCl per 10 μL of DUQ solution.

For the assay, 20 μL of DUQH_2 is added to 930 μL of HEPES buffer (40 mM HEPES, 20 mM NaCl, pH 7.4) and 70 μL of the reconstituted vesicles (0.15 μM protein, 6.57 mM lipid/polymer). The oxidation of DUQH_2 to DUQ ($\epsilon_{275\text{nm}} = 12.25 \text{ mM}^{-1} \text{ cm}^{-1}$ in aqueous solution) is monitored at 275 nm for 5 minutes.

The relative activity of cytochrome bo_3 is calculated by converting the absorbance reading at 275 nm into μmol (μM) of DUQH_2 and then plotting this against time. The gradient of the initial 20 s of the curve is calculated ($\mu\text{M}\cdot\text{s}^{-1}$). The first measurement is taken as full activity (100%) after which the relative activity is measured as a function of storage time.

Hybrid vesicle characterisation results

We have previously demonstrated successful reconstitution of cytochrome bo_3 in hybrid vesicles, quantifying membrane activity by spectroscopic assay of decylubiquinol oxidation [34]. As a redox-active proton pump, another key function that can be assayed is the transmembrane proton motive force that the protein can generate. This can be achieved by encapsulation of a pH-sensitive fluorescent probe inside these vesicles, HPTS. Firstly, however, we must establish whether hybrid membranes can maintain a transmembrane pH difference by not being excessively leaky to protons. We quantify membrane proton permeability by adjusting the extravesicular pH by ± 0.5 pH units through addition of HCl or NaOH: the rate of change of pH inside the vesicles is then monitored.

The time-dependent change in internal pH following NaOH/HCl addition for POPC liposomes to $\text{PBd}_{22}\text{-PEO}_{14}$ polymersomes in 25 mol% $\text{PBd}_{22}\text{-PEO}_{14}$ increments is presented in Fig. 3 with calculated permeabilities in Table 2. Slow proton leakage with a permeability of $1.1 \pm 0.6 \times 10^{-10} \text{ cm}\cdot\text{s}^{-1}$ (average between +HCl and +NaOH experiments) was measured for POPC liposomes. Polymersomes showed much greater resistance to proton leakage than the lipid bilayer vesicle to the extent that no meaningful permeability could be measured (the error is approximately as large as the measurement). Hybrid vesicles with 25 mol% polymer are found to have a higher permeability than pure liposomes. However 50 mol% and 75 mol% polymer hybrid vesicles are found to be less leaky to protons than the pure lipid membrane, with the latter composition showing an exceptionally low permeability similar to that of the polymersome. To the best of our knowledge, this remarkable insulation against passive proton leakage across a hybrid vesicle membrane is unprecedented. Polymersomes composed of the larger molecular weight $\text{PBd}_{37}\text{-PEO}_{22}$ copolymers have previously been shown to have lower proton permeability than DOPC liposomes, however hybrid vesicles (25% and 50% polymer) in this study were more permeable to protons than the liposomes [40]. In our system, the reduced hydrophobic mismatch between phospholipids and our shorter $\text{PBd}_{22}\text{-PEO}_{14}$ copolymer would appear to significantly reduce defects that permit transmembrane proton passage, resulting in hybrid vesicles of very low proton permeability.

Table 2. Membrane permeabilities measured from a HPTS assay following a shift of ± 0.5 pH units using addition of HCl or NaOH (both are 1.0 M stock solutions).

Vesicle composition	1 M NaOH added		1 M HCl added	
	$P \cdot 10^{11}$ (cm/s)	error $\cdot 10^{11}$ (cm/s)	$P \cdot 10^{11}$ (cm/s)	error $\cdot 10^{11}$ (cm/s)
0	5.5	1.4	16	6
25	11	6	29	9
50	3.3	1.8	17	8
75	1.9	0.3	10	4
100	0.8	0.6	1.8	1.7

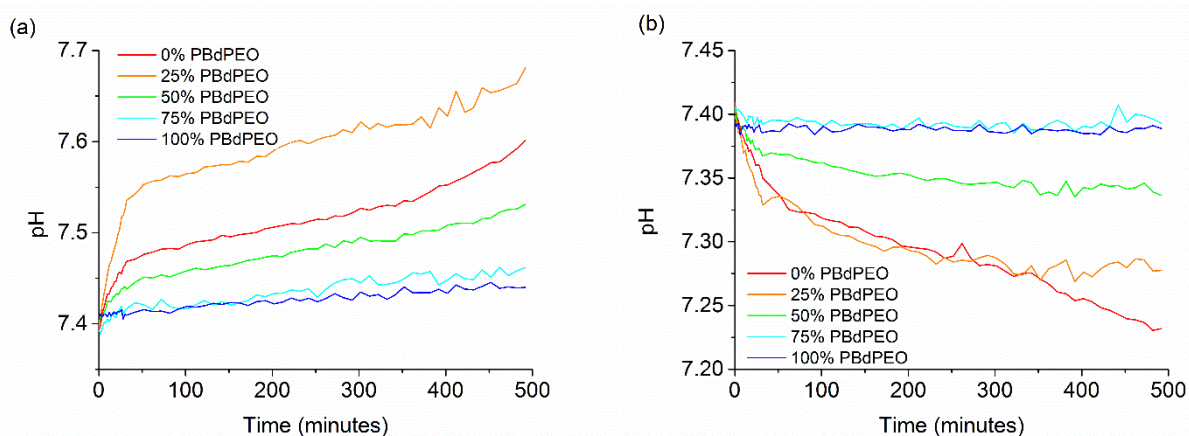


Figure 3. Kinetics of pH change inside vesicles containing HPTS following addition of (a) NaOH and (b) HCl.

We have conducted ensemble spectroscopy studies to characterise the change in pH inside proteo-hybrid vesicles upon addition of the decylubiquinol substrate. Only subtle pH changes have been observed in these experiments across all membrane compositions, we interpret that this is due to random orientation of proteins within these vesicle membranes: based on previous reports, this is not unexpected [41]. The pH shifts that we detect are also much smaller than have been observed for cytochrome bo_3 at the single vesicle level [42]. New reconstitution strategies will need to be developed in order to enhance and control the orientational bias of reconstituted cytochrome bo_3 in hybrid vesicles.

The fundamental benefit of proteo-hybrid vesicles over traditional proteoliposomes is their enhanced functional durability [34]. We have continued to monitor the activity of samples reported in Figure S4 (a period of 42 days) of our previous study [34]. We now have data covering a period of approximately 500 days following sample preparation (Fig. 4). The profound superiority in functional durability of hybrid vesicles is now fully revealed. We use a first order kinetic model to appropriately fit activity (y) data as a function of time (t), excluding the 100% activity on day 0 data points using the equation:

$$y = A \exp(-t/\tau) + B$$

The three fitting parameters amplitude, A , rate constant, τ , and offset, B , are presented in Table 3. The biggest loss in activity occurred within the first week, representative of a proportion of poorly stable enzyme in the sample (approximated as $100 - A - B$): 4% for POPC liposomes, 11% for 50% polymer hybrids and 26% for 75% polymer hybrid vesicles. The subsequent apparent activity half-life ($= \tau \ln 2$) is 18 ± 4 days for POPC liposomes, 83 ± 21 days for 50% hybrid vesicles and 66 ± 11 days for 75% hybrid vesicles. Interestingly, while proteoliposome activity decayed towards zero at long times (B), both hybrid vesicle compositions apparently plateau at approximately 20% of their initial activity. This may suggest some very long-term residual activity is protected within hybrid vesicle formulations. Regardless, maintenance of ~20% of their initial enzymatic activity 500 days after reconstitution in itself is astonishing.

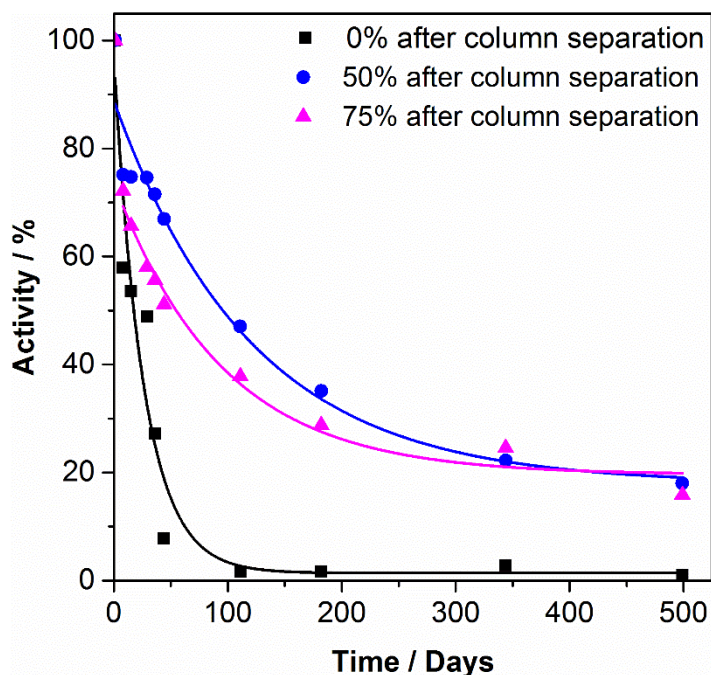


Figure 4. Relative protein activity over time compared to the initial activity after sample preparation for POPC liposomes (0%), 50/50 POPC/PBd₂₂-b-PEO₁₄ hybrids (50%) and 25/75 POPC/PBd₂₂-b-PEO₁₄ hybrids (75%). Data is fitted to a first order kinetic model (see main text for details) with fitting parameters reported in Table 3.

Table 3 Fitting parameters for data in Fig. 4.

Vesicle type	A / %	τ / days	B / %
POPC	95 ± 10	26 ± 6	1 ± 5
50% hybrid	71 ± 6	120 ± 30	18 ± 6
75% hybrid	54 ± 3	95 ± 16	20 ± 2

Summary and Outlook

We have presented a step-by-step protocol for reconstitution of cytochrome bo_3 within hybrid vesicles to aid others in this approach and expanded our material characterisation of these systems. Hybrid vesicles are shown to have exceptional resistance to proton permeability, although the embedded membrane proteins are likely randomly oriented as no significant net proton transport was observed in our experiments. Random orientation will give rise to no consistent net directionality of protein incorporation and thus proton transport within the wider sample, although directionality will often occur at the single vesicle level as our reconstitution protocol is designed to yield an average of one protein per 100 nm vesicle, which we expect to follow a Poisson distribution. Our previous report on these proteo-hybrid vesicles found that 50 mol% PBd-PEO hybrid vesicles comprise the optimal combination of high initial reconstituted activity and long term durability (over 6 weeks). We can now report that these vesicles retain ~20% of their initial activity after 500 days with an activity half-life of approximately 3 months (83 ± 21 days) that preserves significant long-term (non-zero) enzyme activity in these samples.

Our hybrid vesicle compositions have not been optimised. We have not explored the wide parameter space of block copolymer chemistry and molecular weight and partner phospholipid(s) in any noteworthy detail. Therefore, there could be significant room for further improvement of reconstituted

membrane protein durability. We have used a single phospholipid (POPC) in our current investigations for reasons of minimising the compositional complexity to allow for systematic variation and study of membrane properties: we see no reason why other lipids and, in particular, lipid mixtures such as membrane extracts could not be used to further optimise the membrane properties. Furthermore, a very recent report uses a commodity polymer commonly used in cosmetics formulations, PDMS-g-PEO, to functionally reconstitute cytochrome b_0 in pure polymersomes and hybrids with lipids [43], however, no direct evidence is provided for a specific advantage of these vesicles compared to proteoliposomes. The high fluidity of PDMS-g-PEO membranes may give rise to similar problems with fragility that are encountered within liposomes. The higher viscosity of PBd-PEO-rich membranes is very likely to play an important role in stabilising these vesicles and the structure and activity of membrane proteins embedded within them. The PBd hydrophobic block of these polymers is also highly compatible with lipids by forming well-mixed hybrid membranes across compositional parameter space, whereas PDMS-based silicone polymers tend to demix from lipids across a significant range of compositional space. The prospects for hybrid vesicles in membrane protein technologies are compelling and is likely to be a vibrant area of subsequent future investigation.

Acknowledgements

RS, MR and PAB acknowledge support from EPSRC Centre for Doctoral Training in Soft Matter and Functional Interfaces (EP/L015536/1). EM and PAB thank the BBSRC CBMNet network for vacation scholarship D0121. LJCJ was funded by the European Research Council under the European Union's Seventh Framework Programme (FP/2007–2013)/ERC Grant Agreement no. 280518.

References

- [1] Y. Arinaminpathy, E. Khurana, D.M. Engelman, M.B. Gerstein, *Drug Discovery Today*, 14 (2009) 1130-1135.
- [2] S.H. White, W.C. Wimley, *Annual Review of Biophysics and Biomolecular Structure*, 28 (1999) 319-365.
- [3] D.M. Engelman, *Nature*, 438 (2005) 578-580.
- [4] K.R. MacKenzie, *Chemical Reviews*, 106 (2006) 1931-1977.
- [5] A.M. Seddon, P. Curnow, P.J. Booth, *Biochimica Et Biophysica Acta-Biomembranes*, 1666 (2004) 105-117.
- [6] T.H. Bayburt, S.G. Sligar, *Febs Letters*, 584 (2010) 1721-1727.
- [7] J.L. Popot, in: R.D. Kornberg, C.R.H. Raetz, J.E. Rothman, J.W. Thorner (Eds.) *Annual Review of Biochemistry*, Vol 792010, pp. 737-775.
- [8] S.C. Lee, T.J. Knowles, V.L.G. Postis, M. Jamshad, R.A. Parslow, Y.P. Lin, A. Goldman, P. Sridhar, M. Overduin, S.P. Muench, T.R. Dafforn, *Nature Protocols*, 11 (2016) 1149-1162.
- [9] J.L. Rigaud, D. Levy, *Liposomes*, Pt B, 372 (2003) 65-86.
- [10] D. Marquardt, B. Geier, G. Pabst, *Membranes*, 5 (2015) 180-196.
- [11] E. Sezgin, I. Levental, S. Mayor, C. Eggeling, *Nat. Rev. Mol. Cell Biol.*, 18 (2017) 361-374.
- [12] D. Lingwood, K. Simons, *Science*, 327 (2010) 46-50.
- [13] J.E. Goose, M.S.P. Sansom, *Plos Computational Biology*, 9 (2013).
- [14] M. Javanainen, H. Hammaren, L. Monticelli, J.H. Jeon, M.S. Miettinen, H. Martinez-Seara, R. Metzler, I. Vattulainen, *Faraday Discussions*, 161 (2013) 397-417.
- [15] G.J. Doherty, H.T. McMahon, *Annual Review of Biophysics*2008, pp. 65-95.
- [16] J. Lemiere, F. Valentino, C. Campillo, C. Sykes, *Biochimie*, 130 (2016) 33-40.
- [17] A.A. Gurtovenko, I. Vattulainen, *Biophysical Journal*, 92 (2007) 1878-1890.
- [18] S.J. Marrink, F. Jahnig, H.J.C. Berendsen, *Biophysical Journal*, 71 (1996) 632-647.
- [19] K.T. Powell, J.C. Weaver, *Bioelectrochemistry and Bioenergetics*, 15 (1986) 211-227.

- [20] B.M. Discher, Y.Y. Won, D.S. Ege, J.C.M. Lee, F.S. Bates, D.E. Discher, D.A. Hammer, *Science*, 284 (1999) 1143-1146.
- [21] C. LoPresti, H. Lomas, M. Massignani, T. Smart, G. Battaglia, *Journal of Materials Chemistry*, 19 (2009) 3576-3590.
- [22] M. Garni, S. Thamboo, C.-A. Schoenenberger, C.G. Palivan, *Biochimica et Biophysica Acta (BBA) - Biomembranes*, 1859 (2017) 619-638.
- [23] P.A. Beales, S. Khan, S.P. Muench, L.J.C. Jeuken, *Biochemical Society Transactions*, 45 (2017) 15-26.
- [24] J.F. Le Meins, C. Schatz, S. Lecommandoux, O. Sandre, *Materials Today*, 16 (2013) 397-402.
- [25] J. Nam, P.A. Beales, T.K. Vanderlick, *Langmuir : the ACS journal of surfaces and colloids*, 27 (2011) 1-6.
- [26] M. Chemin, P.M. Brun, S. Lecommandoux, O. Sandre, J.F. Le Meins, *Soft Matter*, 8 (2012) 2867-2874.
- [27] D. Chen, M.M. Santore, *Soft Matter*, 11 (2015) 2617-2626.
- [28] T.P.T. Dao, A. Brulet, F. Fernandes, M. Er-Rafik, K. Ferji, R. Schweins, J.P. Chapel, F.M. Schmutz, M. Prieto, O. Sandre, J.F. Le Meins, *Langmuir : the ACS journal of surfaces and colloids*, 33 (2017) 1705-1715.
- [29] S. Lim, H.-P. de Hoog, A. Parikh, M. Nallani, B. Liedberg, *Polymers*, 5 (2013) 1102.
- [30] J. Nam, T.K. Vanderlick, P.A. Beales, *Soft Matter*, 8 (2012) 7982-7988.
- [31] A. Olubummo, M. Schulz, R. Schops, J. Kressler, W.H. Binder, *Langmuir : the ACS journal of surfaces and colloids*, 30 (2014) 259-267.
- [32] M. Schulz, W.H. Binder, *Macromolecular Rapid Communications*, 36 (2015) 2031-2041.
- [33] S. Winzen, M. Bernhardt, D. Schaeffel, A. Koch, M. Kappl, K. Koynov, K. Landfester, A. Kroeger, *Soft Matter*, 9 (2013) 5883-5890.
- [34] S. Khan, M.Q. Li, S.P. Muench, L.J.C. Jeuken, P.A. Beales, *Chemical Communications*, 52 (2016) 11020-11023.
- [35] E.R. Geertsma, N.N. Mahmood, G.K. Schuurman-Wolters, B. Poolman, *Nature protocols*, 3 (2008) 256-266.
- [36] H.R. Marsden, C.B. Quer, E.Y. Sanchez, L. Gabrielli, W. Jiskoot, A. Kros, *Biomacromolecules*, 11 (2010) 833-838.
- [37] P.M. Frederik, D.H.W. Hubert, in: N. Duzgunes (Ed.) *Liposomes*, Pt E2005, pp. 431-+.
- [38] J.D. Robertson, L. Rizzello, M. Avila-Olias, J. Gaitzsch, C. Contini, M.S. Magoń, S.A. Renshaw, G. Battaglia, *Scientific Reports*, 6 (2016) 27494.
- [39] J.N. Rumbley, E.F. Nickels, R.B. Gennis, *Biochimica et Biophysica Acta (BBA)-Protein Structure and Molecular Enzymology*, 1340 (1997) 131-142.
- [40] W.F. Paxton, P.T. McAninch, K.E. Achyuthan, S.H.R. Shin, H.L. Monteith, *Colloids and Surfaces B: Biointerfaces*, 159 (2017) 268-276.
- [41] A. Puustinen, M. Finel, T. Haltia, R.B. Gennis, M. Wikstrom, *Biochemistry*, 30 (1991) 3936-3942.
- [42] M.Q. Li, S. Khan, H.L. Rong, R. Tuma, N.S. Hatzakis, L.J.C. Jeuken, *Biochimica Et Biophysica Acta-Bioenergetics*, 1858 (2017) 763-770.
- [43] L. Otrin, N. Marušič, C. Bednarz, T. Vidaković-Koch, I. Lieberwirth, K. Landfester, K. Sundmacher, *Nano Letters*, 17 (2017) 6816-6821.